DOI: https://doi.org/10.1016/j.autcon.2021.103894

Actuation methods for deployable scissor structures

Carlos J. García-Mora*, Jose Sánchez-Sánchez[a]
* Architectural technology team, Department of Building Structures and Geotechnical Engineering, Higher Technical School of Architecture of Seville, Seville University
Av. de la Reina Mercedes, 2, 41012 Seville, Spain
email@carlosjosegarciamora.com

[a] Architectural technology team, Department of Building Structures and Geotechnical Engineering, Higher Technical School of Architecture of Seville, Seville University

Abstract

The use of techniques to automate the deployment process of deployable structures has always been of prominent interest for architects, engineers and designers of these mechanical systems. The fact of being "deployable" in itself implies a simple way of assembling the structure and this assembly is even more promising if it can be achieved by pressing a button. The first part of this scientific paper is focused on a brief description of the different techniques already used by other authors to automate the deployment of structures. After that, 4 techniques to deploy a structure are proposed where each one is analysed and applied to a deployable structure with straight rods and a cylindrical shape. Finally, some of these applications are built and their behaviour with respect to the theoretical model is checked.

Keywords: Deployable structure, scissor mechanism, folding, straight rod, geometry, kinematics, bistable, automation, technical solutions, actuation methods

1. Introduction

The deployable structure of scissors is a mechanism just composed of rods and joints and where its behaviour can be compared with a crank mechanism with an increase in the length of the rods [1] [2]. The sequential union of these mechanisms allow the creation of deployable structures with complex geometries [3].

From a historic point of view, scissors can be divided into 3 types (bistable and non-bistable) [4] [5] in function of the shape of the rods and the orientation. The first type is called "translational units" (Figure 1 a) [6] and its main property is that the focal distances (the distance between the extreme joints of the rods of a scissor that is pointing to the deployment centre of the structure [7]) are always parallel during the whole deployment process (blue discontinuous lines in the following figure). The second type is called "polar units" [8] (Figure 1 b) and its principal property is that focal distances are not parallel not only during the deployment process but also in the structure's final position. They will be only parallel in the folded position when their rods are simplified as lines (without thickness) [9].

The last type of scissors is called "angular units" (Figure 1 c) [10] [11]. The main difference between the previous cases and this design is the configuration of the rods: translational units and polar units have straight rods and angular units have bended rods. Consequently, focal distances will never be parallel.

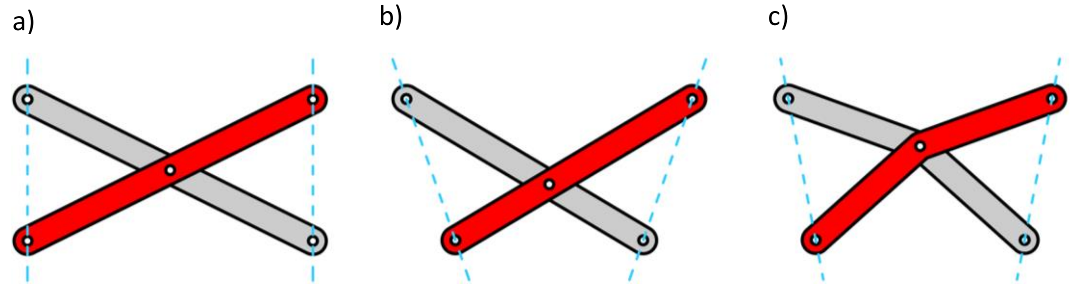

Fig. 1. Classification of the types of scissors.

The combination of these modules using different geometric strategies and mathematical tools allows the creation of deployable geometries with a high level of complexity [12] [13]. Traditionally, these structures are deployed manually between many people and being careful with respect to possible misalignments [14]. However, in case of big deployable structures (concerts, auditoriums, etc.) [15] or systems where manual access is not possible (spatial systems) [16] [17], this type of deployment is not suitable. To solve this situation, many automatic techniques to enhance this process have been developed. The first case that is going to be presented is the use of wires [18]. The trajectory of this wire will go through the focal distances and when somebody pulls the cable, the structure will be folded (Figure 2).

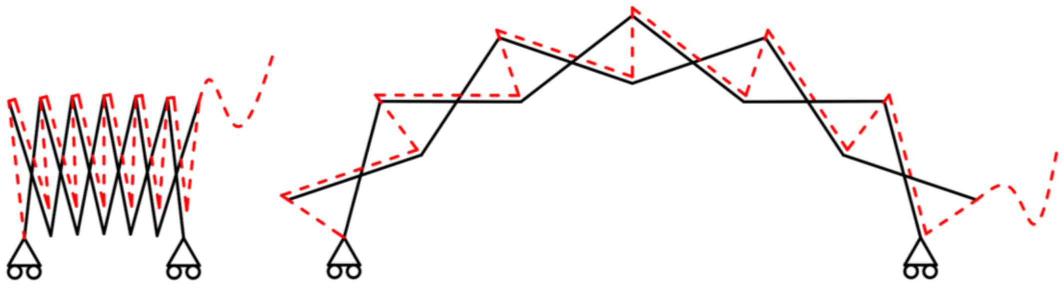

Fig. 2. Semi-automatic deployment process of a scissor structure using a wire.

One of the first authors who developed a technology to automate the deployment process was Emilio Pérez Piñero with his project “Mobile Theatre” (Teatro Ambulante) (Figure 3) [19] [20]. This work was composed of a central tower and the deployable structure was unfolded using a simple linear movement (like the mechanism of an umbrella). This structure was presented for the first time in the VI Symposium of the International Union of Architects (London) and it was labelled as a “highly important technical contribution with a notable simplicity and with a possibility of immediate realization” by the jury of the Symposium (Félix Candela, Buckminster Fuller, etc.) [21] [22].

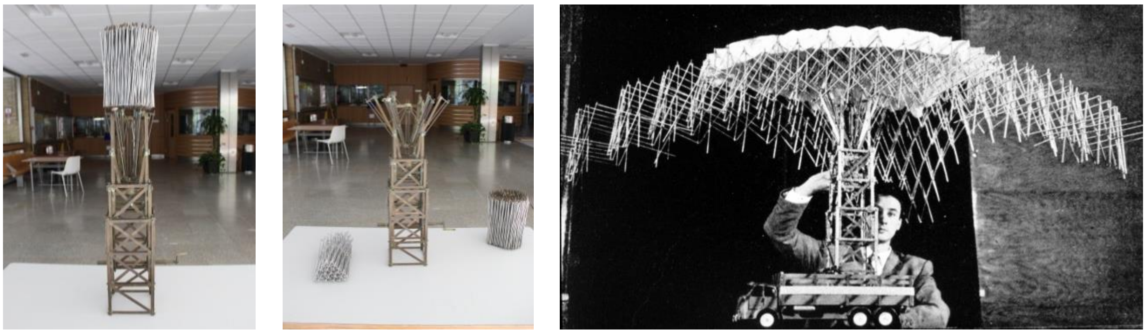

Fig. 3. Mobile Theatre by Emilio Pérez Piñero.

After that, other authors such as Chuck Hoberman, began to use more advanced techniques for the automatic deployment of big structures. One of his most important projects in this field was the deployable stage for the 2002 Salt Lake City Olympic Games [23]. The goal was to design an automatic deployable stage with an iris shape where the shape can be regulated according to the type of celebration. Once the structure has been completely assembled, the last steps are the lighting and the facility of the automatic system. The final result is represented in Figure 4.

Fig. 4. Deployment process of the stage.

Another project that requires an automatic system due to its size is the mobile cover of the auditorium from Jaén (Spain) [24] [25]. This project was designed and built by Architects Félix Escrig Pallares and Jose Sánchez-Sanchez in 01/07/1998. This structure uses bended rods as a basic element and the final geometry has the shape of a cylinder. The result is a structure with only one direction of deployment and with an arch shape in the folded position (Figure 5).

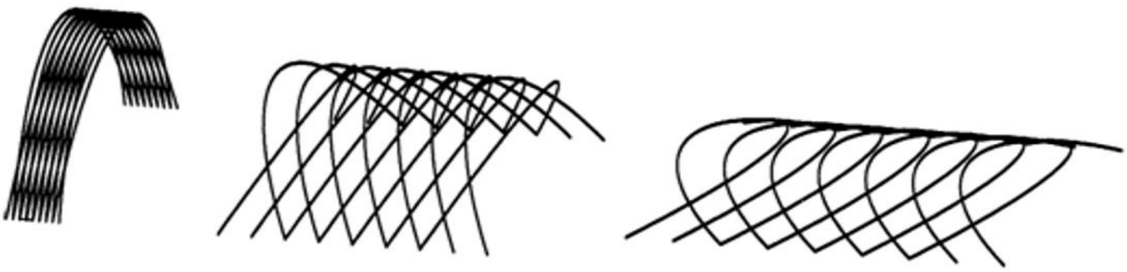

Fig. 5. Deployment process of the structure designed by Félix Escrig Pallarés and Jose Sánchez-Sanchez

Once the theoretical model has been completed, a reduced-scale prototype was built to check its behaviour during the deployment process (Figure 6). The results were quite satisfactory and there were not excessive deformations. The next step was to design and build the automation of the structure. This mechanism was based on two rails with a linear displacement that allowed the support of the deployable structure. This system was moved using an electrical motor, a gear box and some end stops (Figure 6). Finally, a textile was used to cover the structure and the interior space of the auditorium was designed.

Fig. 6. Verification of a reduced-scale structure module, automatic mechanism and final result.

An additional deployment technique that has been used by the previous authors and with a common application in the deployable structure field is the gravity deployment system. An example of this case is the structure of San Pablo Olympic Pool in Seville (two spheres of 900 m^2 each one), where the deployment process was achieved using a crane, the weight of the structure and some cables (Figure 7) [26].

Fig. 7. Gravity deployment system in San Pablo pool (Seville).

The next project can be observed in Figure 8 [27]. The geometry of this structure is from the restaurant “Los Manantiales” in Xochimilco, México (architect: Felix Candela). Once the structure of rods was built, the automation process was developed using two stepper motors. The first one was connected with a threaded rod and it allowed the deployment of the structure between 0% and 90%. It was not possible to achieve 100% due to the use of elastic joints in the structure: These joints are really easy to be manufactured but they have the behaviour of a spring and if the quantity is considerable, they will provide a high force against the folded position of the structure. The stepper motor of the threaded rod could not provide enough force to balance the influence of the elastic joints. Consequently, to improve the deployment process from 90% to 100%, a second stepper motor was used in combination with some wires. The whole deployment process is represented in Figure 8.

Fig. 8. Deployment process of the geometry “Los Manantiales” in Xochimilco, Mexico (Author: Félix Candela).

Although most of the previous examples are applied in the field of architecture [28] [29] [30] [31], there are also other fields where deployment automation technology is very important, for example, aerospace engineering [32]. In this context can be also found the figure of Emilio Pérez Piñero and his relationship with NASA. In 1969, Emilio and Félix Candela travelled together to the NASA facilities with the goal of building greenhouses on the Moon using deployable structures. Emilio designed an auto deployable dome adapted to moon vehicles, but the project was not built.

Later, Félix Candela received a letter from the “Department of the Navy: Naval Facilities Engineering Command” of the US showing a prominent interest in the dome of Piñero for a project in Antarctica. However, the letter was intercepted by Mexican authorities and arrived a month later. When Emilio developed the project (Figure 9 a), the answer was too late. Returning to the present, one of the most important projects in deployable space technology can be found in the “Large European Antenna” (Figure 9 b and c) [33]: a deployable structure for earth observation, telecom, and military purposes.

The shape of this reflector is obtained using the concept of a truss antenna. This antenna has 3 elements: a reflector cable truss, some elastic tie cables to form the shape and the supporting structures. This system can be deployed using an auxiliary mechanism or deployable beams.

a) b) c)

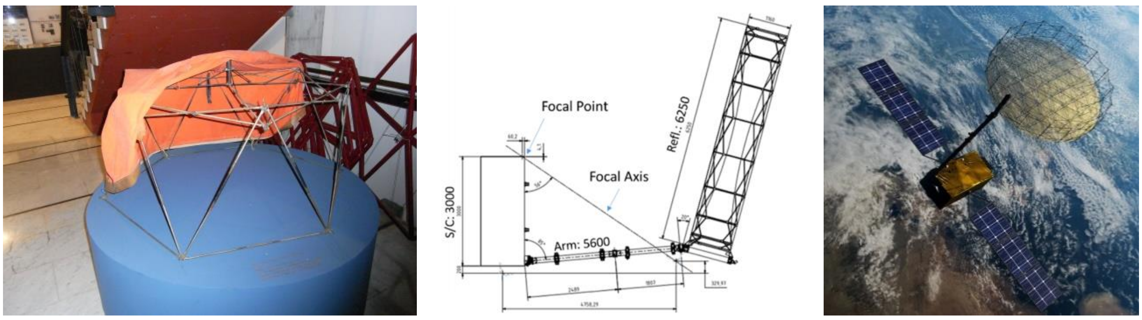

Fig. 9. (a) Deployable structure designed by Piñero for the Department of the US Navy; (b) General drawing of the Large European Antenna; (c) Render of the Large European Antenna.

2. Methodology

The methodology of this research is the following:

- Step 1 (construction method): An introduction to the proposed technique is developed and the main construction elements will be described.
- Step 2 (theoretical behaviour): The behaviour of the constructive solution will be analysed from a physical / mathematical point of view in order to obtain the output parameters (motor power, piston force, etc.) based on the input parameters (friction coefficient, geometric design variables, etc.).
- Step 3 (application case): A practical application of the corresponding constructive solution will be designed. With the aim of homogenising the applications, all the deployable techniques developed in this article will be applied to a cylindrical deployable structure with translational units and with the design of Figure 10.

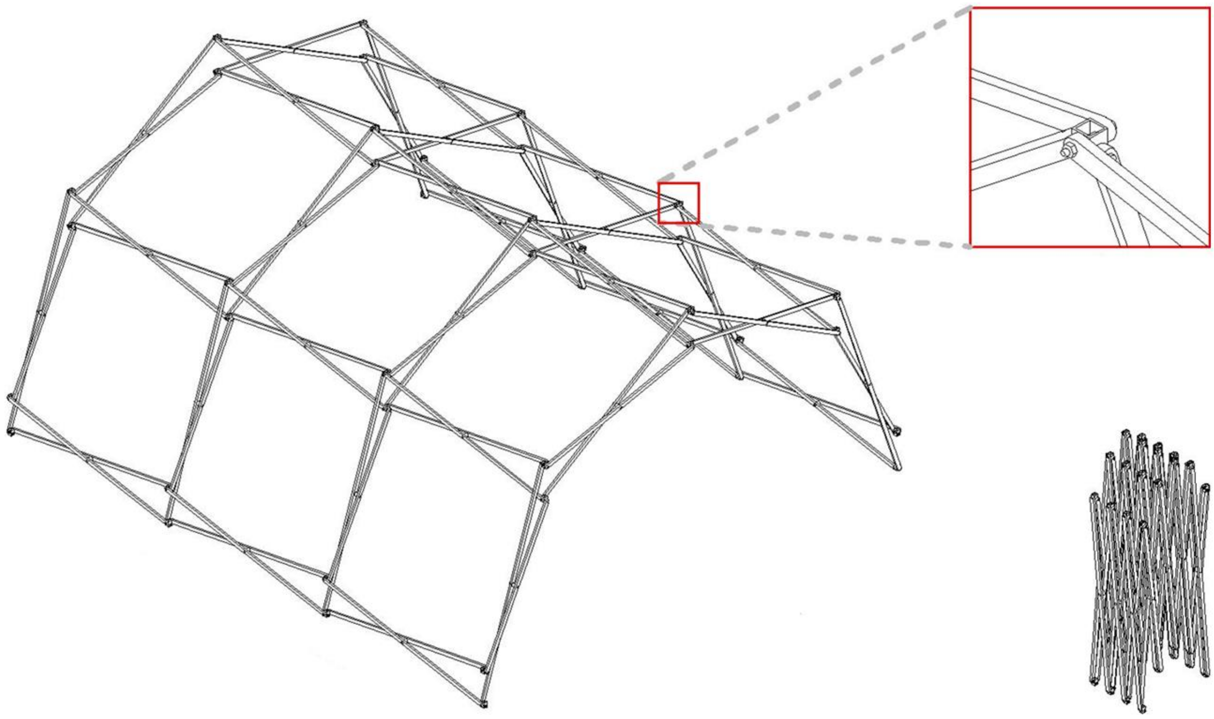

Fig. 10. Deployable structure where the techniques developed are going to be applied.

- Step 4 (practical behaviour): The constructive solution will be built when economic and technical conditions are suitable.
- Step 5 (advantages and disadvantages): Taking as a reference the information developed in the previous sections, the main advantages and disadvantages of the corresponding deployment technique will be presented from a technological point of view.

3. Deployment techniques developed

3.1. Motors in the focal directions

3.1.1. Construction method

This deployment technique involves the use of threaded rods and motors with the axis positioned in the direction of the focal lengths of the deployable structure. Additionally, rods may be used as guides to avoid the torsion of the structure due to the torque of the motors (if the weight of the structure is high enough, these rods may be omitted). The constructive drawing has been represented in Figure 11.

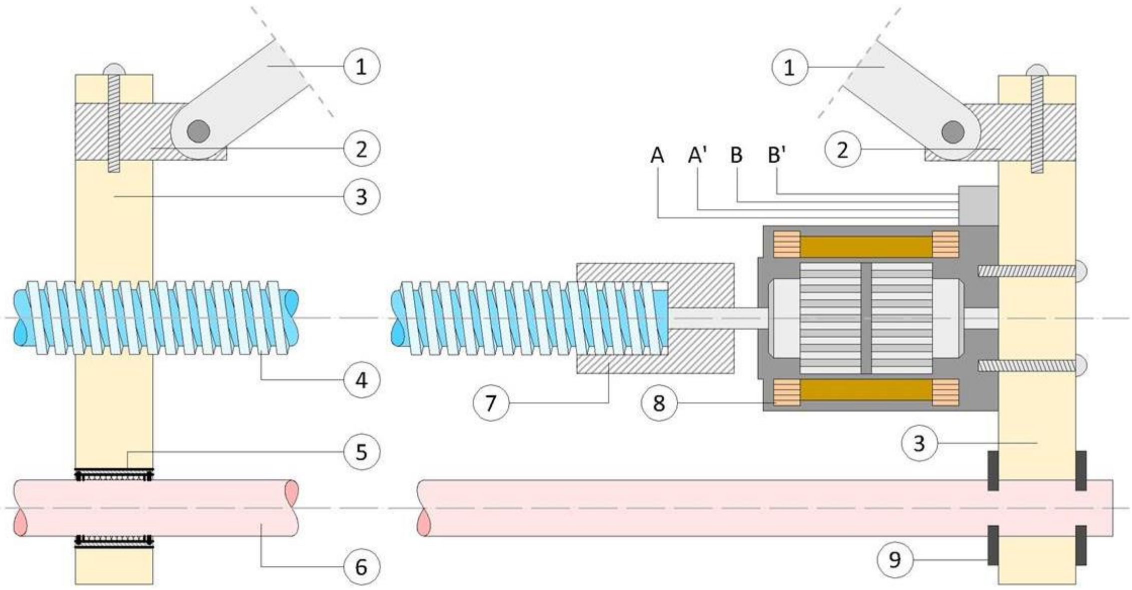

Fig. 11. Constructive drawing of the use of motors in the focal directions.

As can be observed in Figure 11, the automatic deployment system has two supports (3). In each support, an extreme of the rod of each scissor (1) will be connected for the deployment of the structure. Also, each rod will be connected to the corresponding support with an articulated joint (2). The deployable movement is achieved using the rotation of a motor (8), which can be a stepper motor, servomotor, continuous current motor, etc. (in this case, a stepper motor has been chosen). The rotation of this motor is transmitted to a threaded rod (4) which is attached to the motor using a flex coupler (7). Optionally, a rod can be used as a guide (6) to reduce the torque that the structure will experience during the motor's working time. The extreme of this rod is fixed in one of the supports with a snap retaining ring (9) and the other extreme can slide using a linear bearing (5).

In the case of using a continuous current motor or an alternating current motor, the behaviour of the motor will be limited by an end stop. Likewise, if the motor is a servomotor, its control is relatively simple since the motor parameters will be indicated in the datasheet. However, if the motor is a stepper motor (coil 1 = A-A' and coil 2 = B-B'), its control is a bit more complex because it requires the use of an external electronic support. The prototype developed has been designed using a stepper motor with the electronic board and the signal sequence represented in Figure 12.

a)

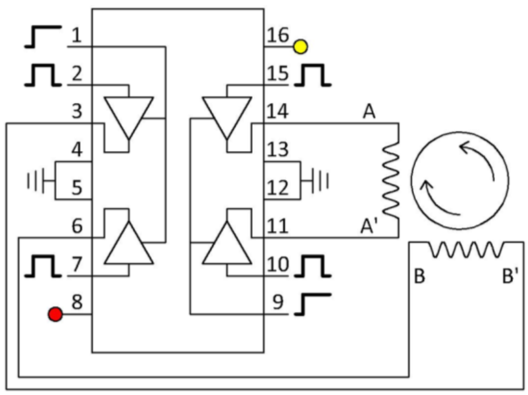

b)

	A	A'	B	B'
1	1	0	0	1
2	1	1	0	0
3	0	1	1	0
4	0	0	1	1

c)

	A	A'	B	B'
1	1	0	0	1
2	1	0	0	0
3	1	1	0	0
4	0	1	0	0
5	0	1	1	0
6	0	0	1	0
7	0	0	1	1
8	0	0	0	1

Fig. 12. (a) Control of a stepper motor using a H-bridge. The red circle is the power supply of the motor and the yellow circle is the power supply of the electronic device; (b) Stepper motor control sequence using full–step; (c) Stepper motor control sequence using half–step.

3.1.2. Theoretical behaviour

The calculation model that reproduces the mechanical behaviour of this deployment system can be summarised in the superior support. In this part, the following forces are represented (Figure 13):

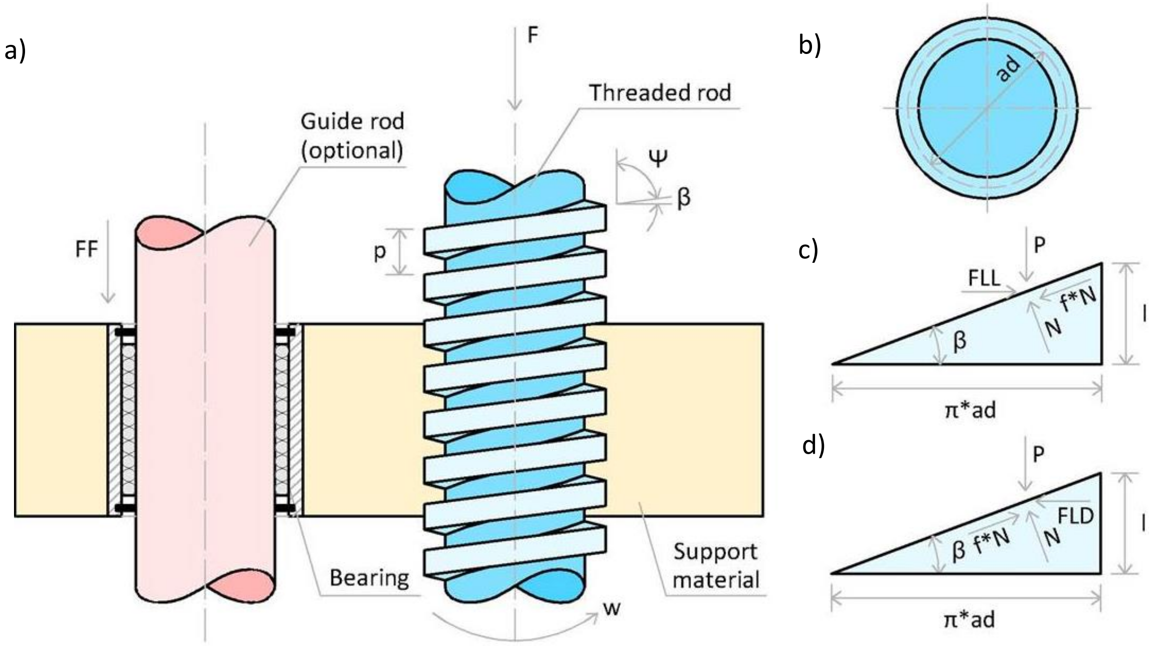

Fig. 13. (a) Generic description of the mechanism; (b) Average diameter of the threaded rod; (c) Diagram of forces on the threaded rod (load lifted); (d) Diagram of forces on the threaded rod (load lowered).

Where:

a) F = Weight of the load to move.
b) FF = Frictional force on the guide rod.
c) P = Summation of the forces in the direction of the threaded rod.
d) p = Pitch of the threaded rod.
e) Ψ = Helix angle of the threaded rod.

f) β = Advance angle of the threaded rod.
g) ad = Average diameter of the threaded rod.
h) f = Coefficient of friction of the threaded rod.
i) N = Normal force with respect to the surface.
j) l = Advance of the threaded rod.
k) FLL = Force (load lifted).
l) FLD = Force (load lowered)
m) w = Angular speed of the threaded rod.

If a balance of horizontal forces is applied in Figure 13 c):

$$FLL - f \cdot N \cdot cos(\beta) - N \cdot sin(\beta) = 0 \tag{1}$$

With respect to vertical forces:

$$-P - f \cdot N \cdot \sin(\beta) + N \cdot \cos(\beta) = 0 \tag{2}$$

If a balance of horizontal forces is applied in Figure 13 d):

$$-FLD + f \cdot N \cdot cos(\beta) - N \cdot sin(\beta) = 0 \tag{3}$$

With respect to vertical forces:

$$-P + f \cdot N \cdot \sin(\beta) + N \cdot \cos(\beta) = 0 \tag{4}$$

The equation of FLL and FLD are obtained using Eq. (1), Eq. (2), Eq. (3) and Eq. (4):

$$FLL = P \cdot \frac{f \cdot cos(\beta) + sin(\beta)}{cos(\beta) - f \cdot sin(\beta)} \quad and \quad FLD = P \cdot \frac{f \cdot \cos(\beta) - \sin(\beta)}{f \cdot \sin(\beta) + \cos(\beta)} \tag{5}$$

On the other hand, the torque for the load lifted is:

$$TLL = FLL \cdot \frac{ad}{2} \tag{6}$$

And the torque for the load lowered is:

$$TLD = FLD \cdot \frac{ad}{2} \tag{7}$$

$$\beta = \frac{l}{\pi \cdot ad} \quad and \quad P = \left|\vec{F} + \overrightarrow{FF}\right| \tag{8}$$

If Eq. (6), Eq. (7) and Eq. (8) are replaced in Eq. (5), the final equations for the torque are obtained:

$$TLL = \left|\vec{F} + \overrightarrow{FF}\right| \cdot \frac{ad}{2} \cdot \left(\frac{\pi \cdot f \cdot ad + l}{\pi \cdot ad - f \cdot l}\right) \tag{9}$$

$$TLD = \left|\vec{F} + \overrightarrow{FF}\right| \cdot \frac{ad}{2} \cdot \left(\frac{\pi \cdot f \cdot ad - l}{\pi \cdot ad + f \cdot l}\right) \tag{10}$$

It is important to highlight that Eq. (9) can only be applied if a square thread is used. In the case of other types of threads, for example Acme threads, the friction parameters must be divided by $\cos(\beta)$. For a square thread, the torque when the load is lifted is:

$$TLL = \left|\vec{F} + \overrightarrow{FF}\right| \cdot \frac{ad}{2} \cdot \left[\frac{\pi \cdot f \cdot ad \cdot \sec(\beta) + l}{\pi \cdot ad - f \cdot l \cdot \sec(\beta)}\right] \tag{11}$$

Finally, the power given by the motor will be:

$$P_u = \frac{Threaded\ rod\ power}{\eta_r \cdot \eta_{tr}} \tag{12}$$

Where:

$$Threaded\ rod\ power = P \cdot Displacement\ speed\ of\ the\ load \tag{13}$$

$$\eta_r = Efficiency\ of\ the\ gear\ reductor\ (datasheet) \tag{14}$$

$$\eta_{tr} = Efficiency\ of\ the\ threaded\ rod = \frac{TLL(f=0)}{TLL} = \frac{\left|\vec{F} + \overrightarrow{FF}\right| \cdot l}{2 \cdot \pi \cdot TLL} \tag{15}$$

Furthermore, a power balance must be done in order to obtain the power in the input of the motor (P_i):

$$P_i = U_i \cdot I_i \begin{cases} P_e \begin{cases} P_H \\ P_m \\ P_u \end{cases} \\ P_J = R \cdot I_i^2 \end{cases} \tag{16}$$

Where:

a) P_e = Internal electrical power
b) P_J = Power lost due to the Joule effect
c) P_H = Power lost in the electromagnetic core ≈ $0.05 \cdot P_u$
d) P_m = Power lost due to mechanical reasons (datasheet) = $0.2 \cdot P_u$
e) R = Resistor of the wire of the coil

Consequently:

$$P_i = P_e + P_J = P_H + P_m + P_u + P_J \tag{17}$$

Finally:

$$I_i = C_1 \cdot C_2 \cdot C_3 \cdot C_4 \cdot \frac{U_i - \sqrt{U_i^2 - 5 \cdot R \cdot P_u}}{2 \cdot R} < I_{imax\ of\ the\ motor} \tag{18}$$

Where:

a) C_1 = The security coefficient due to the friction between the wheels and the ground = 2
b) C_2 = The security coefficient due to the misalignment during the deployment process = 1.5
c) C_3 = The security coefficient due to the irregularity of the ground = 1.25

c) C_4 = The security coefficient due to the friction of the joints = 2

Security coefficients have been obtained developing comparisons between the theoretical approach and the built model.

3.1.3. Application case

The next step is to apply the previous theoretical development to the deployable structure studied. To do so, it is important to highlight that the manufacturing process available is laser cutting and the construction material will be MDF with a thickness of 3 mm. The prototype designed has one stepper motor in each corner of the structure and in the rest of the external support a wheel will be used. Likewise, the rod guide has been removed. The final design can be observed in Figure 14.

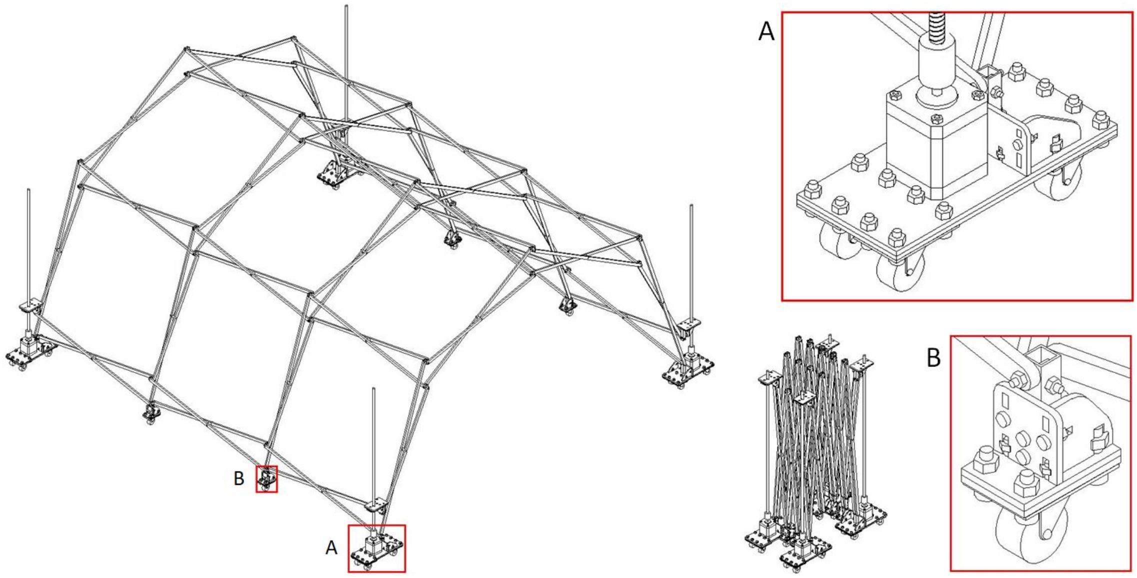

Fig. 14. Model designed using motors in the focal direction.

Once the design has been completed, the prototype is built. The structure in folded and unfolded positions is represented in Figure 15.

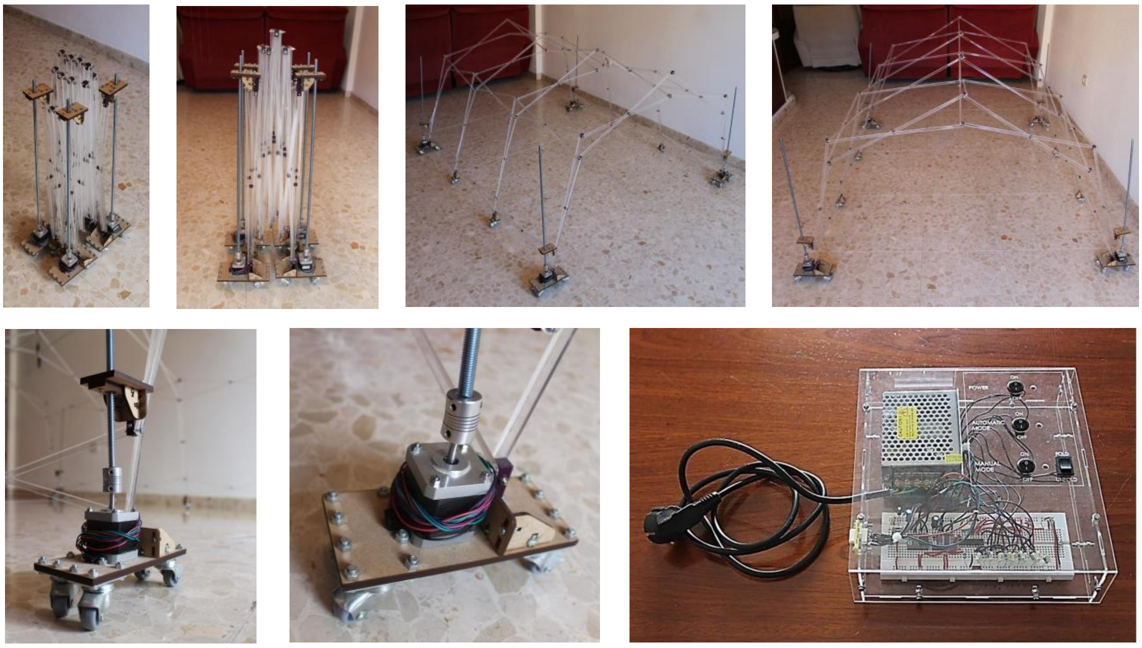

Fig. 15. Folded and unfolded positions of the built structure using stepper motors in the focal directions and the electronics required.

3.1.4. Practical behaviour

In our case, the family of motors that has been used is the NEMA family. A table with the most noteworthy properties of these motors can be seen in Table 1.

Motor name	Resistor	U_i	I_{imax}	Weight	Used
NEMA 14	4.00 Ω	12.00 V	0.80 A	0.18 kg	No
NEMA 17	2.10 Ω	12.00 V	1.20 A	0.35 kg	Yes
NEMA 23	1.50 Ω	24.00 V	2.40 A	1.00 kg	No
NEMA 34	0.40 Ω	36.00 V	6.30 A	3.85 kg	No

Table 1. Most important properties of the NEMA family motors.

The rest of the parameters are:

- η_r = 1 (there is not a gear box)
- Displacement speed of the support material = 0.01 m/s
- l = 0.00125 m
- ad = 0.0075 m
- f = 0.2
- FF = 0 (there is not a guide rod)
- P = F =10kg / 4 = 2.5 kg (using influence area and considering the worst case)

If the equations of the theoretical approach are applied, the evolution of each motor can be obtained (Fig. 16). In our case, the model that has been used is the NEMA 17 and the comparison between the results from the equations and the experiments are quite similar.

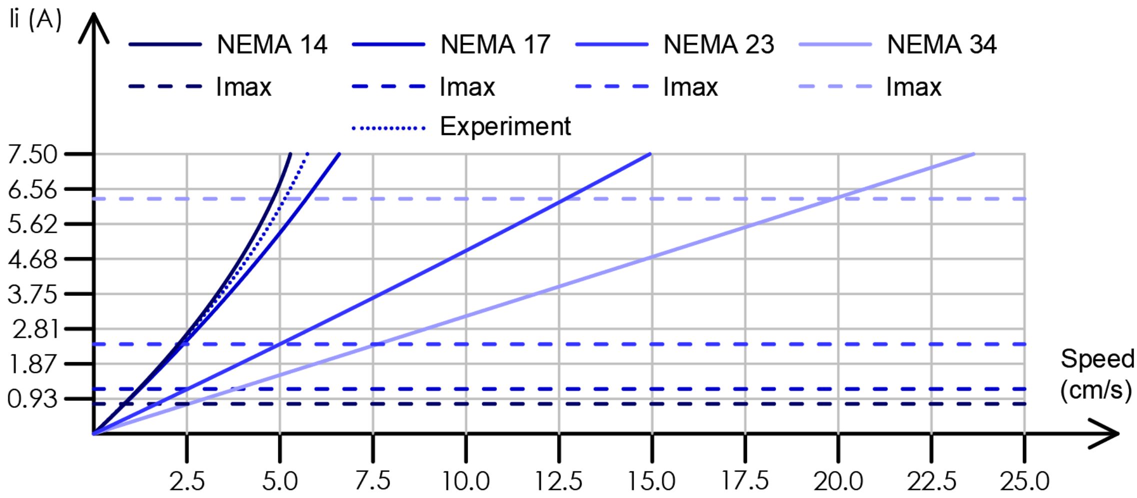

Fig. 16. Evolution of the current in the motor input versus the movement speed of the focal distance of the deployable structure for each model of the NEMA motor family.

As can be observed in Figure 16, the theoretical curve and the experimental curve almost coincide for small speeds and, in consequence, for speeds associated with currents below the maximum intensity, the proposed theoretical model can be considered as valid.

3.1.5. Advantages and disadvantages

a) Advantages:

a1) This automatic system not only works in translational units but also in polar units because its application only depends on the focal distance.
a2) There is a high commercial availability of the components of this technique and, consequently, several solutions (motor power, electronic device, etc.) can be studied for the same structure.
a3) The deployment speed can be controlled with a high resolution if stepper motors are used. In the case of any other type of motor (DC, AC, etc.) the final position of deployment must be obtained using displacement sensors (end stop).

b) Disadvantages:

b1) The structure will have some threaded rods in the folded position that can be a drawback during transport due to collisions or obstacles.
b2) This technique is not suitable if the structure has a high weight because the threaded rods have a low efficiency.
b3) If the distance between supports and the number of scissor modules is high, it will be necessary to use motors not only on the extreme supports of the structure but also on the middle joints to avoid a loss of force during the deployment process. These motors will have an important role in the deformation of the structure according to its weight. Consequently, this technique is suitable for deployable structures with an effective area up to 20 m^2 and with an effective height up to 2.5 m.

3.2. Motors in the middle point of a scissor

3.2.1. Construction method

The goal of this deployment technique is to obtain the movement of the scissors using a motor on the middle joint of the rods. Since the space used by the motor should not have a strong influence on the folding of the structure, the motors must have a large diameter and a low height. Commercially, these motors are called "pancake motors" and they can be purchased as servo motors or as stepper motors. An example of these motors working as servo motors can be observed in Figure 17.

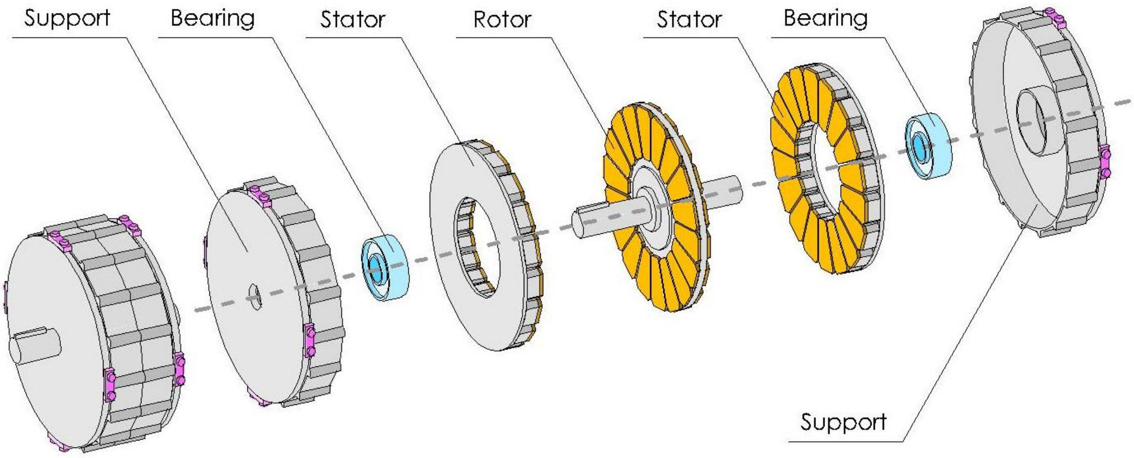

Fig. 17. Perspective view and exploded view of a pancake servo motor.

As mentioned above, the space used by the motor must not affect the deployment of the structure. Consequently, the motors will be placed between the rods of each scissor. In this union between the scissor and the motor, one of the rods will be fixed to the motor shaft and the other rod will be free. This design is represented in Figure 18.

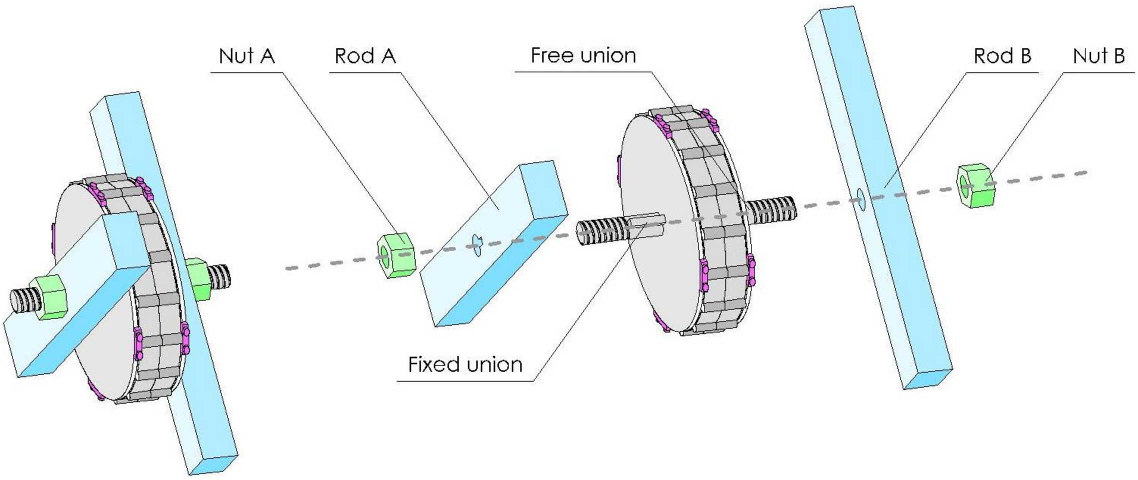

Fig. 18. Perspective view and exploded view of the union between the motor and the rods.

3.2.2. Theoretical behaviour

The working process of this technique has been represented in Figure 19. The application of a rotational movement in the middle joint of the scissors (with a fixed extreme and a free extreme) allows the appearance of a couple of forces at the ends of each rod. These forces will originate a chain effect ending with the deployment of the structure.

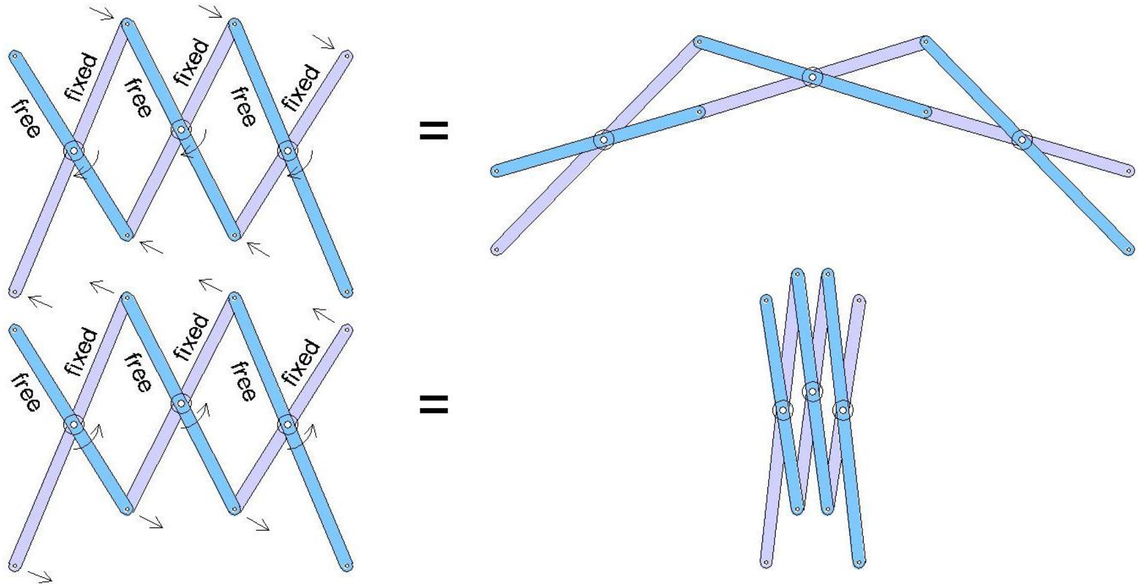

Fig. 19. Transmission of forces in the structure due to the behaviour of the motor.

3.2.3. Application case

In Figure 20, the motors have been positioned only in the longitudinal direction of the structure. In the rest of the modules it will not be necessary to use more motors because the average size of the structure avoids an excessive loss of the transmission of forces. It is important to highlight that the motor has to fit in the space between the rods of the same scissor and that it will have a considerable influence in the last steps of the structure's deployment, limiting the final size of the packaging (Figure 20).

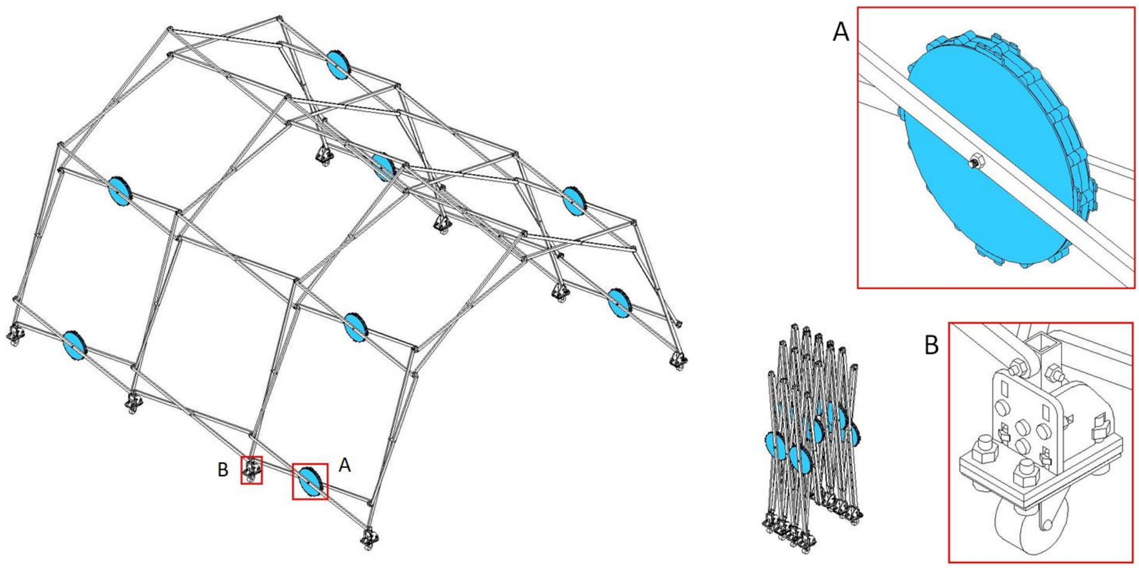

Fig. 20. Use of pancake servo motor in a cylindrical deployable structure.

3.2.4. Advantages and disadvantages

a) Advantages:

a1) If the motors do not have a high diameter, the whole system is quite compact.
a2) The transmission of forces using a rotation in the scissors is more efficient from the vector decomposition point of view in comparison with applying a force at the focal distance of the scissor.

b) Disadvantages:

b1) The motors are moved with the structure during deployment process and, consequently, the mass to be moved is influenced by the weight of the motors.
b2) The behaviour of each motor must be specific for each type of scissor: not all motors will rotate the same degrees and at the same speed.
b3) This system does not allow compensating forces due to the misalignment between the motor shaft and the structure.
b4) The size of the joints must be enough to keep the motors (between 2 cm and 6 cm of thickness in function of commercial models). Consequently, the effective area of the structure should be from 10 m^2 to 30 m^2 and the effective height from 1 m to 3 m.

3.3. Pistons between 2 consecutive scissors

3.3.1. Construction method

The deployment technique that is developed in this section is based on the variation of length between two opposite rods in the union of two different scissors. This variation in length will be absorbed by a linear actuator achieving the control of the deployment. Optionally, auxiliary springs can be placed on some scissors to enhance the deployment process (Figure 21).

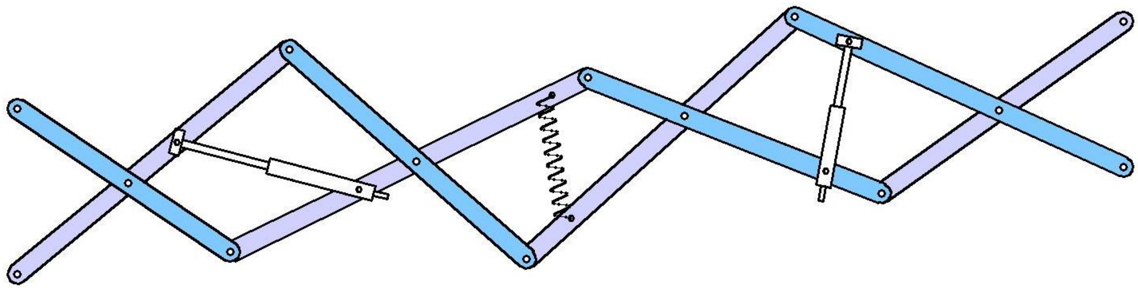

Fig. 21. Set of scissors with a linear actuator and springs (optional) to automate the deployment process.

3.3.2. Theoretical behaviour

The goal is to check if during the whole deployment process of two consecutive scissors, the distance between the extreme points of the piston does not exceed the length of its maximum and minimum length. To figure this out, 2 consecutive scissors are represented in Figure 22.

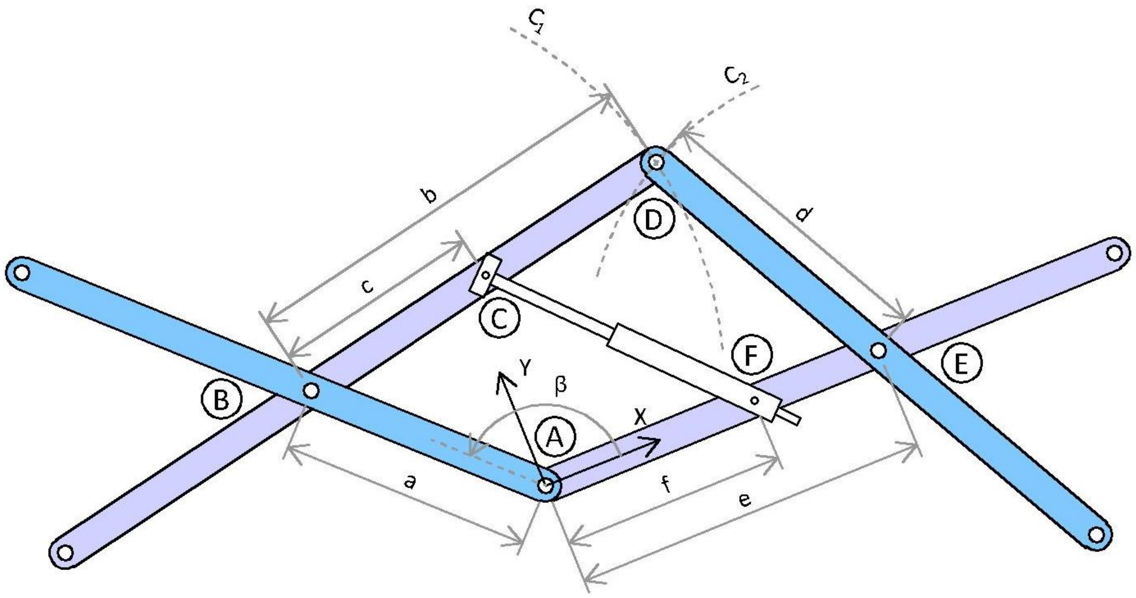

Fig. 22. Two consecutive scissors with all geometric parameters.

Consequently:

- Input parameters: a, b, d, e
- Design parameters: c, f
- Control parameters: β
- Parameter to study: $|\overrightarrow{CF}|$

Where:

$$Circle\ 1: [x - a \cdot \cos(\beta)]^2 + [y - a \cdot \sin(\beta)]^2 = b^2 \quad with \quad 0^o \leq \beta \leq 180^o \tag{19}$$

$$Circle\ 2: [x - e]^2 + [y]^2 = d^2 \tag{20}$$

The next step is to obtain the coordinates of point D. In order to get that, the intersection between Circle 1 and Circle 2 is required:

$$[x - a \cdot \cos(\beta)]^2 + [y - a \cdot \sin(\beta)]^2 + d^2 = b^2 + [x - e]^2 + [y]^2 \tag{21}$$

Variable "y" is cleared:

$$y = \left[\frac{e}{a \cdot \sin(\beta)} - \frac{1}{\tan(\beta)}\right] \cdot x + \frac{a^2 + d^2 - b^2 - e^2}{2 \cdot a \cdot \sin(\beta)} \tag{22}$$

The next step is to replace Eq. (22) in Eq. (20) and to clear the "x" variable. The result is a 2°degree equation:

$$S_1 \cdot x^2 + S_2 \cdot x + S_3 = 0 \tag{23}$$

Where:

$$S_1 = 1 + \left[\frac{e}{a \cdot \sin(\beta)} - \frac{1}{\tan(\beta)}\right]^2 \tag{24}$$

$$S_2 = 2 \cdot \left[\left(\frac{e}{a \cdot \sin(\beta)} - \frac{1}{\tan(\beta)}\right) \cdot \left(\frac{a^2 + d^2 - b^2 - e^2}{2 \cdot a \cdot \sin(\beta)}\right) - e\right] \tag{25}$$

$$S_3 = e^2 - d^2 + \left[\frac{a^2 + d^2 - b^2 - e^2}{2 \cdot a \cdot \sin(\beta)}\right]^2 \tag{26}$$

The positive solution of the previous equation will be always the correct one:

$$x = D_x = \frac{-S_2 + \sqrt{S_2^2 - 4 \cdot S_1 \cdot S_3}}{2 \cdot S_1} \tag{27}$$

In addition:

$$D_x^2 - 2 \cdot e \cdot D_x + e^2 - d^2 + y^2 = 0 \quad with \quad y = D_y \tag{28}$$

If D_y is cleared:

$$D = \left(D_x, D_y\right) = \left[\frac{-S_2 + \sqrt{S_2^2 - 4 \cdot S_1 \cdot S_3}}{2 \cdot S_1}, \sqrt{d^2 - (D_x - e)^2}\right] \quad (29)$$

The last step is to obtain the equation for point C:

$$\overrightarrow{BD} = \frac{\left|\overrightarrow{BD}\right|}{\left|\overrightarrow{BC}\right|} \cdot \overrightarrow{BC} \rightarrow D - B = \frac{b}{c} \cdot (C - B) \rightarrow C = \frac{c}{b} \cdot (D - B) + B \quad (30)$$

Finally, point B is written in function of its Cartesian components:

$$C = \left(C_x, C_y\right) = \left[\frac{c}{b} \cdot (D_x - B_x) + B_x, \frac{c}{b} \cdot \left(D_y - B_y\right) + B_y\right] \quad (31)$$

After this mathematical development, a piston represented in Figure 23 is considered:

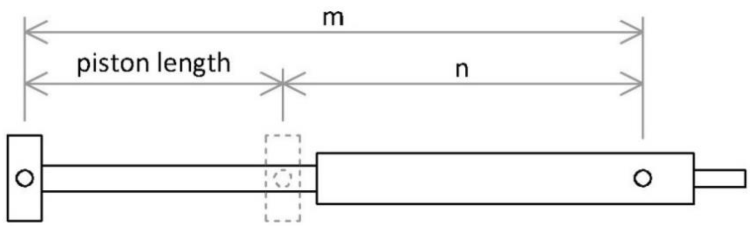

Fig. 23. Standard representation of a linear actuator.

Having Figure 23 as a reference, the next condition must be fulfilled:

$$n \leq \left|\overrightarrow{CF}\right| = \sqrt{(C_x - F_x)^2 + \left(C_y - F_y\right)^2} \leq m \quad (32)$$

If the "n" variable is subtracted from both terms of the previous equation:

$$0 \leq \left|\overrightarrow{CF}\right| - n \leq m - n = piston\ length \rightarrow 0 \leq \left|\overrightarrow{CF}\right| - n \leq piston\ length \quad (33)$$

3.3.3. Application case

The linear actuator has been placed on the perimeter of the structure to avoid possible collisions in the folded position. In the case of a structure with a high quantity of scissors modules, it would also be necessary to place a linear actuator in some intermediate scissors to guarantee the transmission of forces during the deployment process. The result can be observed in Figure 24.

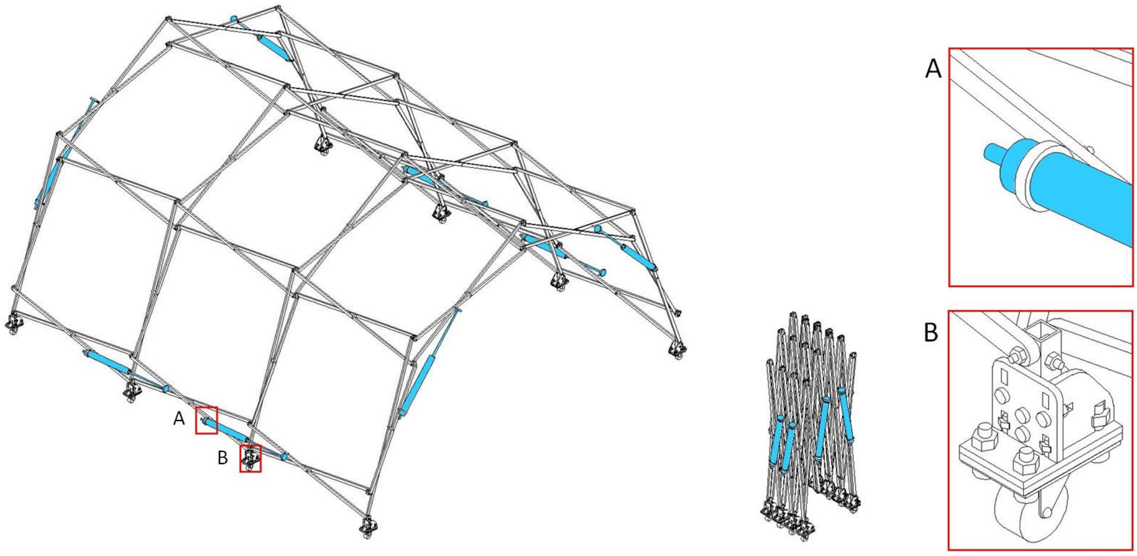

Fig. 24. Cylindrical deployable structure with linear actuators.

The physical construction of a prototype using this technique is not easy because pistons with the length required in the structure designed are only manufactured on an industrial scale and they are therefore expensive. However, and in order to show the working process of this technique of automatic deployment, an application example has been built on a flat structure using a small piston. The results can be observed in Figure 25.

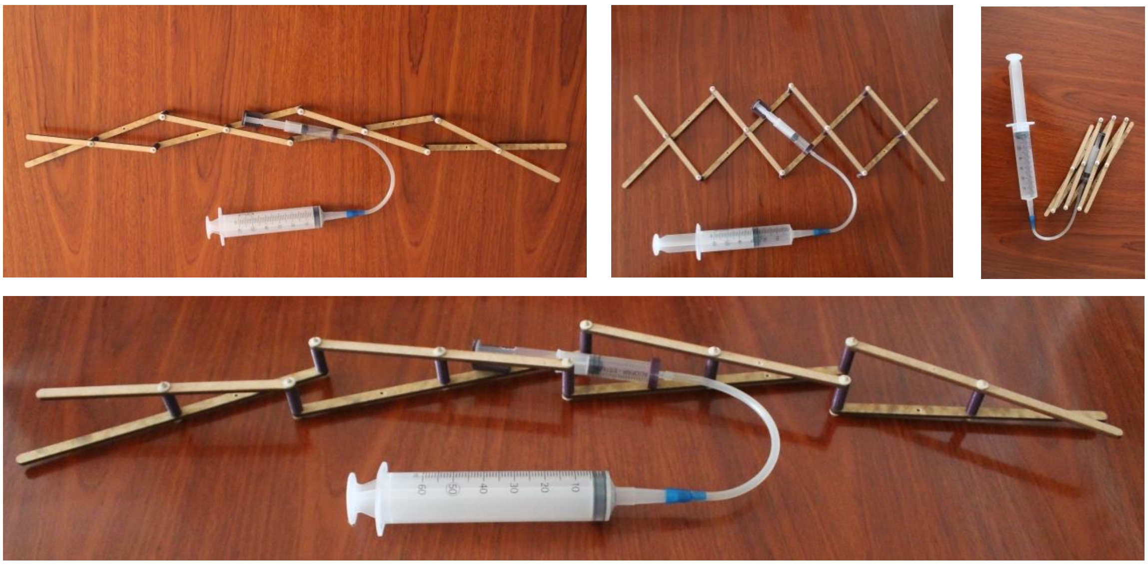

Fig 25. Prototype using a linear actuator between two consecutive scissors.

3.3.4. Practical behaviour

The values of the parameters between 2 scissors in the deployable structure are represented In Table 2:

a	b	d	e	n	piston length
12.5 cm	30.0 cm	37.5 cm	40.0 cm	20.0 cm	18.0 cm

Table 2. Geometric parameters used in the analysis.

By controlling the parameters c and f, the intervals in which the commercial piston is valid for the whole deployment process of the structure are obtained (Table 3):

f=0

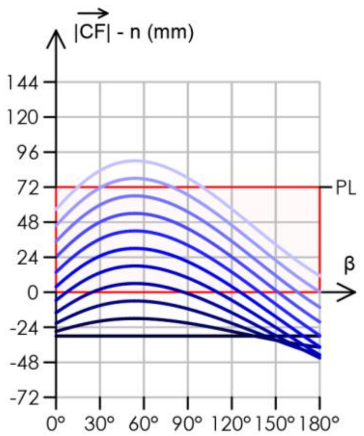

f=(1/3)*e

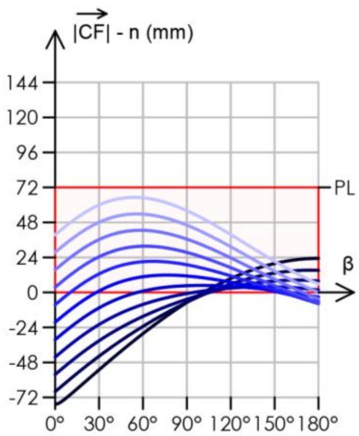

f=(2/3)*e

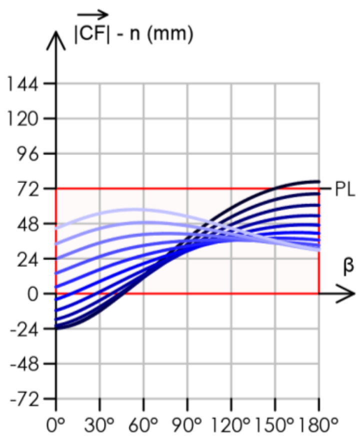

f=e

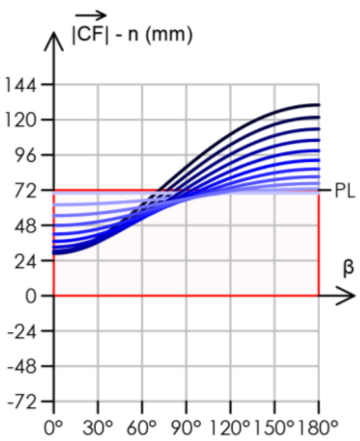

Variables (PL=piston length)			
c=0	c=0.1*b	c=0.2*b	c=0.3*b
c=0.4*b	c=0.5*b	c=0.6*b	c=0.7*b
c=0.8*b	c=0.9*b	c=b	Valid area

Valid ranges			
f=0	f=(1/3)*e	f=(2/3)*e	f=e
Does not exist	c=(0.9*b,b)	c=(0.6*b,b)	c=b

Table 3. Determination of valid working intervals.

3.3.5. Advantages and disadvantages

a) Advantages:

a1) The use of pneumatic or hydraulic energy to control the pistons and the use of a valve that regulates the pressure in a homogeneous way according to the deployed position allows removing any eccentricity of forces during the deployment process.
a2) The union between the linear actuator and the structure does not require a modification of its geometry or of the joints. It is only based on the articulation of both extremes of the linear actuator between two consecutive scissors.

b) Disadvantages:

b1) This technique can only be applied to two scissors that belong to the same plane during the deployment process because the piston geometry cannot be bent. This situation limits the design possibilities and, consequently, it only can be used in flat, cylindrical or translational structures.
b2) The use of a piston between two consecutive scissors that do not belong to the boundary of the structure could increase the size of the structure in the folded position.
b3) If only standard pistons are used, the commercial models allow to design deployable structures with an effective area between 30 m^2 and 40 m^2 and with an effective height between 3 m and 3.5 m.

3.4. Pistons with multiple stages in the focal directions

3.4.1. Construction method

The deployment technique developed in this section involves the use of a multi-stage linear actuator. This linear actuator will be located at the focal lengths of the deployable structure, so the number and the length of each stage will depend on the difference in the focal length between the structure's folded and unfolded position.

In this research, it has been assumed that the deployment of each linear actuator follows a full stage configuration: once one stage of the piston has been deployed, the next is deployed. This behaviour can be achieved using calibrated valves and designing a circulation of the fluid through channels. An example of this approach is represented in Figure 26.

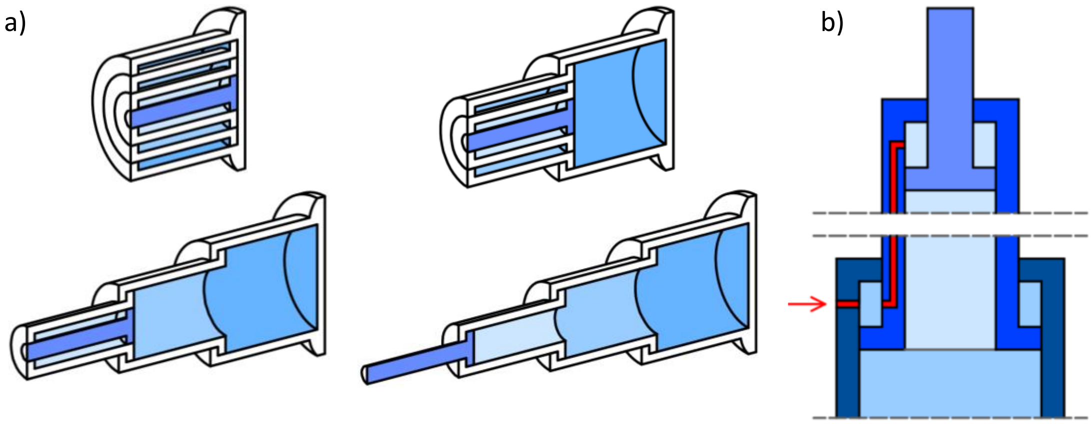

Fig 26. (a) Deployment process of a linear actuator using full stages; (b) Circulation of the control fluid between each stage of the linear actuator.

Another possibility to deploy the linear actuator would be moving all the stages simultaneously. However, this strategy of deployment is more tedious to simulate from a theoretical point of view and, as a result, it has been proposed for future research.

3.4.2. Theoretical behaviour

Before starting with the behaviour study in function of physical parameters, it is necessary to obtain the equations that control the volume changes. The following assumptions will be made:

- The volume of the fluid that circulates through the channels connecting the stages is not considered.
- Power loss due to valves or changes in the direction of the fluid is not considered.
- The thermodynamic process will happen at a constant temperature (isothermal process). Consequently, the temperature will not change during the transition from one stage to the following stage

Likewise, the piston to be studied will have 4 stages (Figure 27).

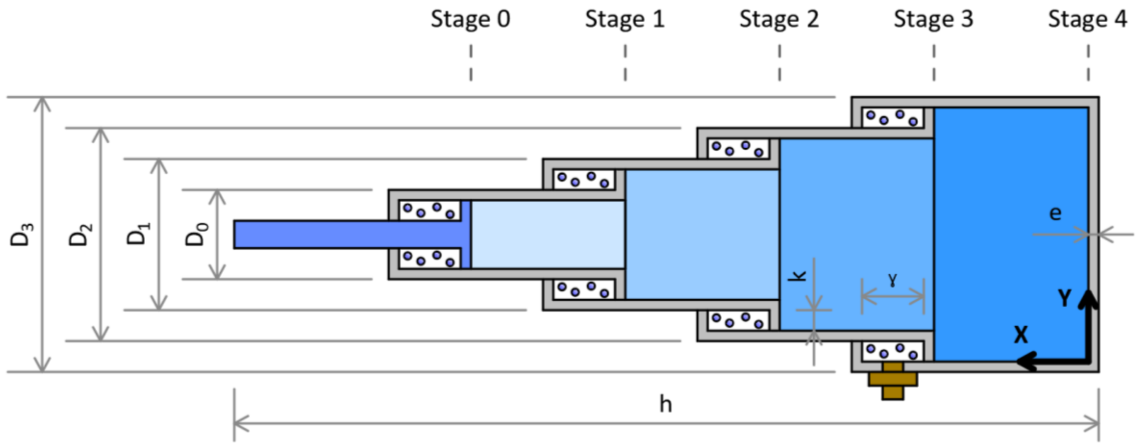

Fig 27. Picture of the multi-stage piston to study.

The concept of work between two consecutive stages can be defined from a physical point of view using the following equation:

$$W_{i,i+1} = F_{i,i+1} \cdot \int_{x_i}^{x} dr = F_{i,i+1} \cdot (x - x_i) \quad with\ i = 0,1,2,3 \ldots\ and\ with\ x_i < x < x_{i+1} \tag{34}$$

Where "F" is the force that is originated by the displacement and "I" is an iterator that indicates the stage to be evaluated. For example, for i = 0 the work will be $W_{0,1}$ = Work due to force $F_{0,1}$ from Stage 0 to Stage 1. On the other hand, to simulate the behaviour of a real gas, the Van der Waals equation will be used:

$$\left[P + a \cdot \left(\frac{n}{V}\right)^2\right] \cdot \left(\frac{V}{n} - b\right) = R \cdot T \tag{35}$$

Where:

a) P = Pressure of the container.
b) V = Volume of the container.
c) T = Temperature of the gas.
d) R = Universal constant of ideal gases
e) n = Number of moles
f) a = Attraction between gas particles
g) b = Available volume of one mole of particles

Another possibility to define the work between two stages of the linear actuator is:

$$W_{i,i+1} = \int_{V_i}^{V} P \cdot dV \quad with\ i = 0,1,2,3 \ldots\ and\ with\ V_i < V < V_{i+1} \tag{36}$$

If Eq. (35) is replaced in Eq. (36):

$$W_{i,i+1} = \int_{V_i}^{V} \left[\frac{n \cdot R \cdot T}{V - n \cdot b} - a \cdot \left(\frac{n}{V}\right)^2\right] \cdot dV = n \cdot R \cdot T \cdot \ln\left|\frac{V - n \cdot b}{V_i - n \cdot b}\right| + a \cdot n^2 \cdot \left(\frac{1}{V} - \frac{1}{V_i}\right) \tag{37}$$

The next step is to combine Eq. (34) with Eq. (37) and to clear the variable of the force:

$$F_{i,i+1} = \left(\frac{1}{x_{i+1} - x_i}\right) \cdot \left[n \cdot R \cdot T \cdot \ln\left|\frac{V - n \cdot b}{V_i - n \cdot b}\right| + a \cdot n^2 \cdot \left(\frac{1}{V} - \frac{1}{V_i}\right)\right] \quad (38)$$

The last step is to rewrite the equations of the volumes in terms of the "x" variable:

$$V_i = \frac{\pi \cdot D_i^2}{4} \cdot x_i \quad and \quad V = \frac{\pi \cdot D_i^2}{4} \cdot x \quad (39)$$

Finally, Eq. (39) is replaced in Eq. (38):

$$F_{i,i+1} = \left(\frac{1}{x - x_i}\right) \cdot \left[n \cdot R \cdot T \cdot \ln\left|\frac{\frac{\pi \cdot D_i^2}{4} \cdot x - n \cdot b}{\frac{\pi \cdot D_i^2}{4} \cdot x_i - n \cdot b}\right| + \frac{4 \cdot a \cdot n^2}{\pi \cdot D_i^2} \cdot \left(\frac{1}{x} - \frac{1}{x_i}\right)\right] \quad (40)$$

It is important to highlight that Eq. 40 only considers the force developed between two consecutive stages and does not consider the force developed by the previous stages. Therefore, this equation must be completed, and the final result is Eq. (41)

$$F_{i,i+1} = \left(\frac{1}{x - x_i}\right) \cdot \left[n \cdot R \cdot T \cdot \ln\left|\frac{\frac{\pi \cdot D_i^2}{4} \cdot x - n \cdot b}{\frac{\pi \cdot D_i^2}{4} \cdot x_i - n \cdot b}\right| + \frac{4 \cdot a \cdot n^2}{\pi \cdot D_i^2} \cdot \left(\frac{1}{x} - \frac{1}{x_i}\right)\right] + \sum_{j=i}^{j=1}\left[F_{j-1,j}\right] \quad (41)$$

The next step will be to apply the previous equation to a theoretical model in order to obtain an idea of how the force developed by the piston would evolve during deployment. The input parameters are represented in Table 4.

a (O_2) (L^2×atm)/mol^2	1.378	D_0 (dm)	1	h (dm)	9
b (O_2) (L/mol)	0.03183	D_1 (dm)	1	e (dm)	0.02
R (L×atm)/(K×mol)	0.08314472	D_2 (dm)	1	k (dm)	0.06
T (K)	295.15	D_3 (dm)	1	Y (dm)	0.2
Molar mass (g/mol)	16	Mass used (g)	0.1	n (mol)	0.00625

Table 4. Input parameters for a 4-stage piston.

If the parameters of Table 4 are used in Eq. (41), the graph of Fig. 28 is obtained.

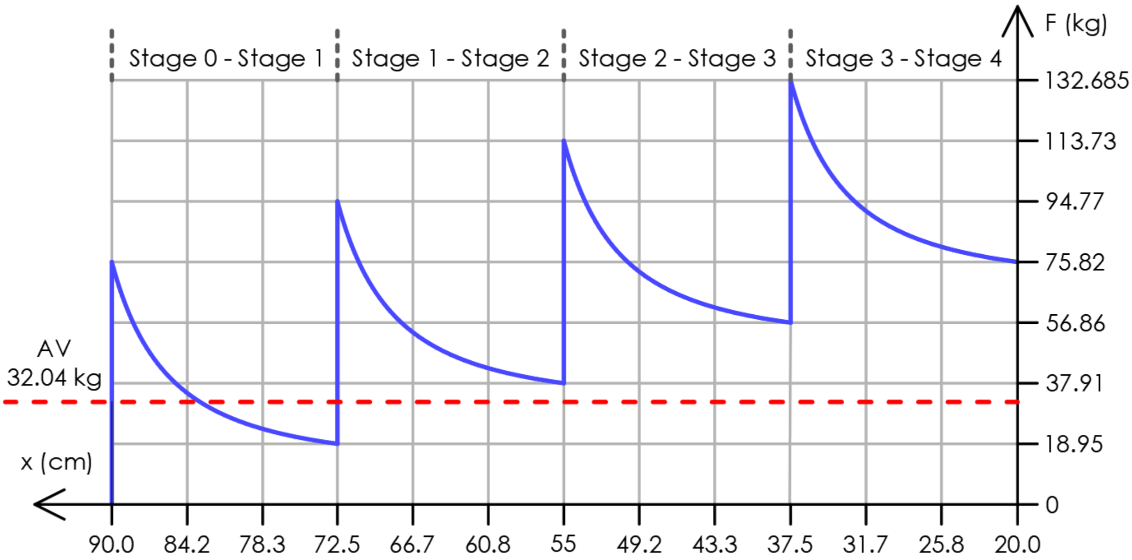

Fig 28. Evolution of the force in a 4-stage piston during the deployment of the structure. AV = Average Value of the force.

From the previous graph, the following conclusions can be obtained:

a) The force during a stage decreases almost exponentially as we approach the next stage.
b) The force developed by one stage is reset when the next stage begins.

The last step would be to graphically represent the force required to deploy the structure in the points where the linear actuator is connected and for the whole deployment process. The automatic deployment process will be correctly designed if the graph of the linear actuator (Figure 28) is always above the graph of the force required to achieve the deployment process.

3.4.3. Application case

The last section applies this multiple-stage linear actuator to this paper's standard structure. A 4-stage linear actuator has been placed in each corner of the structure using the same geometric properties as in the theoretical behaviour. The result can be observed in Figure 29.

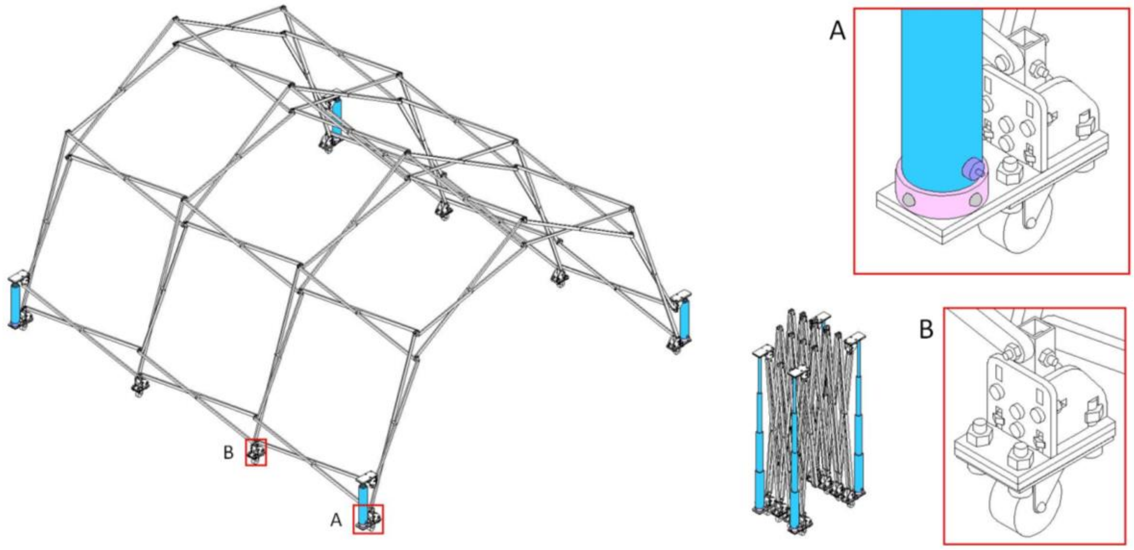

Fig 29. Deployable cylindrical structure with a multiple-stage piston.

3.4.4. Advantages and disadvantages

a) Advantages:

a1) This deployment system allows balancing a possible misalignment of the structure using constant pressure with valves or electrovalves in the linear actuators.
a2) It is commercially viable due to its accessibility in the market.
a3) The geometric design process is simple.

b) Disadvantages:

b1) If the focal distance where the piston is located has a significant variation between the folded and unfolded position of the structure, the piston will have many stages and the price of the deployable system will increase considerably. This situation means that the length of the rods should be between 75 cm and 150 cm (deployable structures with an effective area between 30 m^2 and 40 m^2 and with an effective height between 3 m and 3.5 m)
b2) A pump is required to achieve the deployment process.

4. Application to larger scales

In case of larger scales, it would be necessary to perform a study based on the force that will be supplied by the automation technique for all deployment positions, for example, running a simulation of the deployment process. The results of this study shall be balance using ponderation coefficients in function of the security level, the type of the loads and the rugosity of the ground where the structure will be deployed.

Consequently, the use of automation techniques in large scale deployable structures is going to depend on:

- The height of the structure: If the structure is very tall in the unfolded position, the movement of the gravity centre of the deployable structure during the deployment process will require that the automation technique provides a higher force.
- The commercial availability and price of the components: If the length of the rods is higher than 2 m, the price of all pistons and motors can have an important influence in the price of the structure.

5. Conclusions

The need of automation of the deployment process rising due to the impossibility of doing this manually for reasons of size, human resources, etc. After the development of this research about how to achieve this goal, it can be deduced the following conclusions:

- Motors in the focal directions: Simple solution based on a high commercial availability of the components but it is not recommendable when the distance between supports is higher than 4 m due to the loss of force during the deployment process.

- Motors in the middle point of a scissor: Efficient solution with a good decomposition of the vectors of force but the joints must have enough size to keep the motors.

- Pistons between 2 consecutive scissors: They can be used for a wide range of deployable structures sizes and the eccentricity can be removed due to the use of pneumatic energy. However, this technique can only be applied to two scissors that belong to the same plane during the deployment process.

- Pistons with multiple stages in the focal directions: Deployable technique that can also remove the eccentricity. However, this technique has limits in terms of the number of stages of the pistons.

From this perspective, the most effective method to put deployable structures in motion is the use of pistons between 2 consecutive scissors because it has not a considerable influence in the design of the structure and the use of pneumatic energy allows a self-controlled deployment process.

6. Formatting of funding sources

Research funded by Performance Ideas y Aplicaciones SL (Performance Ideas and Applications SL)

7. References

[1] A. Fomin, L. Dvornikov, M. Paramonov, A. Jahr, To the theory of mechanisms subfamilies, in: International Conference on Mechanical Engineering, Automation and Control Systems 2015 (MEACS2015) 124, 2015, pp. 1–7, https://doi.org/10.1088/1757-899x/124/1/012055

[2] A. Fomin, L. Dvornikov, J. Paik, Calculation of general number of imposed constraints of kinematic chains, in: International Conference on Industrial Engineering 206, 2017, pp. 1309–1315, https://doi.org/10.1016/j.proeng.2017.10.636

[3] F. Escrig, Modular, Ligero, Transformable: Un Paseo Por La Arquitectura Ligera Móvil (modular, light, transformable: a walk through mobile lightweight architecture), Seville Unviersity, Sevilla, 2012 (ISBN: 9788447214273)

[4] L.I.W. Arnouts, T.J. Massart, N. De Temmerman, P.Z. Berke, Computational modelling of the transformation of bistable scissor structures with geometrical imperfections, Engineering Structures. 117 (2018), pp. 409–420, https://doi.org/10.1016/j.engstruct.2018.08.108

[5] L.I.W. Arnouts, T.J. Massart, N. De Temmerman, P.Z. Berke, Multi-objective optimisation of deployable bistable scissor structures, Automation in Construction, Volume 114, 2020, pp. 1–14, ISSN 0926-5805, https://doi.org/10.1016/j.autcon.2020.103154

[6] K. Roovers, N. De Temmerman, Deployable scissor grids consisting of translational units, International Journal of Solids and Structures. 121 (2017), pp. 45–61, https://doi.org/10.1016/j.ijsolstr.2017.05.015

[7] C. J. García-Mora, J. Sánchez- Sánchez, Geometric method to design bistable and non -bistable deployable structures of straight scissors based on the convergence surface, Mechanism and Machine Theory, 146 (April 2020), pp. 1–31, https://doi.org/10.1016/j.mechmachtheory.2019.103720

[8] K. Roovers, N. De Temmerman, Geometric design of deployable scissor grids consisting of generalized polar units Journal of the International Association for Shell and Spatial Structures. 58 (2017), pp. 227–238, https://doi.org/10.20898/j.iass.2017.193.865

[9] C. J. García-Mora, J. Sánchez-Sánchez, The convergence surface method for the design of deployable scissor structures. *Automation in Construction*. University of Seville, February 2021, vol. 122, pp. 1–19, https://doi.org/10.1016/j.autcon.2020.103488

[10] C. Hoberman, 1991. Radial expansion/retraction truss structures. US Patent. Number: US5024031A, https://patents.google.com/patent/US5024031A/en

[11] S. Krishnan, Y. Li, Geometric design of deployable spatial structures made of three-dimensional angulated members, Journal of Architectural Engineering, 26 (2020), pp. 20–29, https://doi.org/10.1061/(asce)ae.1943-5568.0000416

[12] F. Escrig, J.P. Valcárcel, Geometry of expandable space structures, International Journal of Space Structures, 8 (1993), pp. 71–84, https://doi.org/10.1177/0266351193008001-208

[13] F. Escrig, Arquitectura Transformable (transformable architecture), Seville Higher Technical School of Architecture, 1993, pp. 95–124 (ISBN: 9788460085836)

[14] F. Escrig-Pallarés, J. Pérez-Valcárcel, J. Sánchez-Sánchez, Two way deployable spherical grids, International Journal of Space Structures, 11 (1996), pp. 257–274, https://doi.org/10.1177/026635119601-231

[15] J. Pérez-Valcárcel, M. Freire Tellado, M. Muñoz Vidal, Estructuras desplegables para actividades lúdicas (deployable structure for recreational activities), Revista de investigación y arquitectura contemporánea, 9 (2019), pp. 129–146, https://doi.org/10.17979/bac.2019.9.0.4635

[16] M. Arya, J. F. Sauder, R. Hodges, S. Pellegrino, Large-Area Deployable Reflectarray Antenna for CubeSats. Aerospace Research Central (ARC). January 2019, pp. 1–11, https://doi.org/10.2514/6.2019-2257

[17] Y. Akgün, C.J. Gantes, K.E. Kalochairetis, G. Kiper, A novel concept of convertible roofs with high transformability consisting of planar scissor-hinge structures, Engineering Structures, 32 (9) (2010), pp. 2873–2883, https://doi.org/10.1016/j.engstruct.2010.05.006

[18] N. De Temmerman, Design and Analysis of Deployable Bar Structures for Mobile Architectural Applications, Ph.D. thesis, Vrije Universiteit Brussel, 2007. web address (last access: 28 June, 2007 - 17:00), https://www.vub.be/events/2007/design-and-analysis-deployable-bar-structures-mobile-architectural-applications

[19] E. Pérez Piñero: Spanish Patent. Number: GB1009371A, https://worldwide.espacenet.com/patent/search/family/008421768/publication/GB1009371A?q=Collapsible%20reticular%20structure%20EMILIO%20PEREZ%20PINERO

[20] E. Pérez Piñero: US Patent. Number: US3975872A, https://worldwide.espacenet.com/patent/search/family/027240735/publication/US3975872A?q=US3975872A%20PINERO%20EMILIO%20PEREZ

[21] E. Pérez Piñero, Teatros desmontables (deployable theatres), Informes de la Construcción. 24 (June 1971), pp. 34–42, https://doi.org/10.3989/ic.1971.v24.i231.3360

[22] M.C. Pérez Almagro, The photographic file of architect Emilio Pérez Piñero. Structure and documentary analysis, Anal. Document. 20 (2) (2017), pp. 1–16, https://doi.org/10.6018/analesdoc.20.2.277831

[23] C. Hoberman, “Olympic arch”. Salt Lake City, Utah, USA (2002), https://www.hoberman.com/

[24] F Escrig, J. Sánchez. (1999) “Estructura plegable de malla para la cubrición de recintos” (deployable structure for open spaces). Spanish Patent. Number: ES2158787B1, https://patents.google.com/patent/ES2158787B1/es

[25] F. Escrig Pallares, J. Sánchez- Sánchez “Proyecto de cubierta móvil del auditorio descubierto de Jaén” (mobile structure for an auditorium in Jaen). DATE: 01/07/1998, http://www.arquitextil.net/portfolio/auditorium-jaen/

[26] J. Pérez-Valcárcel, F. Escrig Pallares, Recent advances in the analysis of expandable structures, Mobile And Rapidly Assembled Structures, MARAS'96, Seville, 1996, Vol II, pp. 45-54, doi: 10.2495/MRS960041

[27] C. J. García-Mora, J. Sánchez-Sánchez, Our world in a line: Deploying the reality, 60th Anniversary of the International Association for Shell and Spatial Structures (IASS), 2019, pp. 1749-1756, https://www.ingentaconnect.com/content/iass/piass/2019/00002019/00000014/art00013

[28] L. Sánchez-Cuenca, Una Cúpula plegable para la Universidad de Girona (deployable dome for the Girona University), in: EGE Revista de Expresión Gráfica en la Edificación, Number 5, 2008, pp. 91–94, https://doi.org/10.4995/ege.2008.12543

[29] L. Sánchez-Cuenca, Geometric models for expandable structures, Transactions on The Built Environment, 21 (1996) 93–102, https://doi.org/10.2495/MRS960091

[30] L. Alegria Mira, A. P. Thrall, N. De Temmerman, Deployable scissor arch for transitional shelters, Automation in Construction, 43 (July 2014), pp. 123–131, https://doi.org/10.1016/j.autcon.2014.03.014

[31] Lara Alegria Mira, Ashley P. Thrall, Niels De Temmerman, Deployable scissor arch for transitional shelters, Automation in Construction, Volume 43, 2014, pp. 123–131, ISSN 0926-5805, https://doi.org/10.1016/j.autcon.2014.03.014

[32] J. Gantes Charis, Deployable Structures: Analysis and Design, WIT Press, 2001, pp. 1–384 (ISBN: 9781853126604)

[33] Large European Antenna (LEA). Ready for integration by the end of 2020 and for flight in 2021. Companies: High Performance Space Structure Systems GmbH, Large Space Structures GmbH, Ruag Space Germany GmbH, Invent Innovative Verbundwerkstofferealisation Und Vermarktung Neuertechnologien GmbH, INEGI - Instituto De Ciencia E Inovacao Em Engenharia Mecanica E Engenharia Industrial, Von Hoerner & Sulger GmbH, Etamax Space GmbH, Ohb System AG, Airbus Defence And Space GmbH, Ticra Fond, Weber-Steinhaus & Smith, Instituto Nacional De Tecnica Aeroespacial Esteban Terradas, Luma Metall AB, Thales Alenia Space France SAS, https://www.esa.int/ESA_Multimedia/Images/2019/05/HPS_Large_Deployable_Antenna